Applied Catalysis B: Environmental 253 (2019) 49–59

Contents lists available at ScienceDirect

Applied Catalysis B: Environmental

journal homepage: www.elsevier.com/locate/apcatb

Post plasma-catalysis for trichloroethylene decomposition over CeO_2 catalyst: Synergistic effect and stability test

S. Sultana[a,*], A.M. Vandenbroucke[a], M. Mora[b], C. Jiménez-Sanchidrián[b], F.J. Romero-Salguero[b], C. Leys[a], N. De Geyter[a], R. Morent[a]

[a] Research Unit Plasma Technology (RUPT), Department of Applied Physics, Faculty of Engineering and Architecture, Ghent University, Sint-pietersniewstraat 41, B-9000 Ghent, Belgium

[b] Department of Organic Chemistry, Faculty of Sciences, University of Córdoba, Campus de Rabanales, Marie Curie Building, Ctra. Nnal. IV, Km 396, 14071 Córdoba, Spain

ARTICLE INFO

Keywords:
Plasma-catalysis
Trichloroethylene
Cerium oxide
Synergy
Stability

ABSTRACT

This study is devoted to investigate the opportunities of a plasma-catalytic system with CeO_2 downstream (i.e. PPC-Post Plasma-catalysis) for the abatement of trichloroethylene (TCE), a typical chlorinated VOC, from dry air. A multi-pin-to-plate negative DC corona/glow discharge is used and showed poor CO_x selectivity despite having high abatement efficiency due to the formation of oxygenated intermediates such as phosgene, dichloroacetylchloride (DCAC) and trichloroacetaldehyde (TCAA), when operated alone. Nonetheless, NTP enables catalyst activation at lower temperature. As a result, suppression of unwanted chlorinated by-products as well as high CO_x selectivity at lower energy cost have been achieved, proving that this plasma-catalysis route shows great potential as air pollution control technology for low concentrated VOC air streams. Special attention is given to the effect of catalyst temperature, the role of ozone in the plasma–catalytic TCE abatement and the possible synergy between NTP and catalysis. Also, a long term test to evaluate the stability of CeO_2 catalyst has also been successfully performed.

1. Introduction

Environmental air pollution has become a widespread concern as it deteriorates our climate and is harmful for both human and ecological life. Next to NO_x, SO_x, H_2S and particulate matter, volatile organic compounds (VOCs) are a large group of chemical compounds that strongly contribute to poor air quality. Along with their detrimental effect on the environment, they can also cause severe damage on human health due to their toxic, mutagenic or carcinogenic effect [1]. Hence, tightened air quality regulations and increasing environmental awareness act as a driving force for the scientific community to develop new and sustainable air purification technologies to remediate VOC-contaminated air streams.

Extensive studies over the last three decades have been published which ensure that non-thermal plasma (NTP) is a sustainable alternative for conventional technologies such as thermal/catalytic oxidation especially for the treatment of low concentrated VOCs waste gas streams [2,3]. One of the interesting features of this promising technology is the energy selectivity. In an electrical discharge, non-equilibrium plasma is produced in which the delivered energy is selectively consumed to energize electrons instead of heating the entire gas volume. These energetic electrons (1–10 eV) collide with background molecules (N_2, O_2, H_2O) close to room temperature transforming a neutral gas into an ionized state containing a reactive mixture of electrons, ions, radicals, metastables and photons. These reactive energetic plasma species are able to decompose organic compounds to less harmful products (CO_2, H_2O, HX and X_2 with X being a halogen) through cleavage of chemical bonds [4]. Another interesting characteristic of NTP technology is related to the cost-effectiveness, since it can be operated at atmospheric pressure which excludes the use of expensive vacuum equipment. Additionally, the cost per unit pollutant treatment with NTP technology is much lower compared to thermal/catalytic oxidation. Since the chemical reactions in this NTP removal process are highly non-selective, simultaneous removal of different pollutants is another desirable feature of this technology [5–7].

Furthermore, NTP technology can be effectively integrated with other established technologies. In this regard, the combination of NTP with heterogeneous catalysis, referred to as plasma-catalysis, has gained increased interest during the last 20 years [8–11]. Through this hybrid system, the feasibility of NTP technology has been improved by

* Corresponding author.
E-mail address: sharmin.sultana@UGent.be (S. Sultana).

https://doi.org/10.1016/j.apcatb.2019.03.077
Received 11 November 2018; Received in revised form 26 March 2019; Accepted 30 March 2019
Available online 01 April 2019
0926-3373/

enhancing the energy efficiency, carbon mass balance and mineralization degree. The mechanisms that enable a better performance are mainly related to the position of the catalyst either being exposed to the active plasma volume (In Plasma Catalysis-IPC) [12–14] or in close vicinity mainly downstream of the discharge zone (Post Plasma Catalysis-PPC) [15–17]. Interestingly, in both cases, the reactions in the gas phase and on the catalyst surface often add up to induce a synergetic effect on the overall removal efficiency [17–20]. Although IPC has been claimed to be superior to PPC, several studies have however shown enhanced performance of different catalysts in PPC rather than IPC [21–23]. In IPC, both plasma and catalyst simultaneously affect each other, resulting in complex interactions. However, in a two stage process such as PPC, the underlying mechanism is more straightforward while the operating parameters can be separately optimized.

One of the major drawbacks of the NTP technique is the formation of by-products (e.g. ozone, NO_x, secondary degradation products) due to incomplete oxidation, which can be more harmful than the target VOC itself [24–28]. However, a more effective use of NTP is possible by exploiting the oxidative capacity of the harmful ozone molecules by introducing an ozone degrading catalyst downstream of the discharge zone. In this PPC process, long-living ozone molecules produced by plasma are able to reach the catalyst surface, where they decompose and generate active oxygen species which greatly improve the oxidation of both the target VOC and toxic by-products. Moreover, PPC has simpler configuration compared to IPC, which facilitates the replacement of used catalyst in practical application. For these reasons, PPC technology is selected to investigate the feasibility for dilute chlorinated volatile organic compound (CVOC) abatement in this current study.

In the post plasma configuration for the abatement of CVOCs, an environmentally friendly catalyst with appropriate ozone decomposition ability, VOC total oxidation capability (CO_2, H_2O, HCl), hydrothermal stability and specially resistance to chlorine needs to be found. Moreover, it should also have a lower reactive temperature and a stable catalytic performance which stands for the long-term goals of the plasma catalysis process.

Although noble metals (Pd, Pt) [29] are found to be more active than metal-oxide-based catalysts (Mn, Cr, Cu, Ni, Co, Ag) [30] or perovskites regarding CVOC oxidation, their use is however limited by high cost and sensitivity to poisoning especially by chlorine/chloride products [31–34]. Thus, non-noble metal oxide catalysts have been considered as low-cost and environmentally friendly alternatives with better stability for chloro-organics oxidation [35–39]. The desired catalytic properties for effective VOC oxidation are related to redox property, crystal defects, diffusion in the crystal lattice, surface area and high oxygen storage capacity (OSC) and mobility.

In the last decade, the redox properties of ceria (CeO_2) have been intensively analysed. The mechanism of VOC oxidation reactions over ceria is generally considered a redox-type mechanism, in which the key steps are the supply of oxygen by the readily reducible oxide and its re-oxidation by oxygen [40,41]. Moreover, CeO_2 based catalysts (Al_2O_3-CeO_2, Pt/Al_2O_3-CeO_2, CeO_2/HZSM-5) are found to be promising in CVOCs abatement due to a combination of their acidic and oxidizing properties, their thermal stability and resistance to poisoning by chlorine [42,43]. Recently, some researchers studied CeO_2 based catalysts, for the plasma catalytic oxidation of (chlorinated) VOCs [44–47]. To our knowledge, using pure CeO_2 in post plasma catalysis for VOCs abatement is rather limited.

The objective of this current work is to abate TCE (C_2HCl_3) from dry air by combined use of a multi-pin-to-plate negative DC corona/glow discharge with a CeO_2 catalyst downstream. TCE is selected as the target VOC since it is very toxic to our health. According to the International Agency for Research on Cancer (IARC), TCE is carcinogenic to humans, hence its emission into the atmosphere should therefore be reduced [48,49]. Generally, TCE is a chlorinated solvent that is widely used as a degreasing agent in semi-conductor and metal industry. Recently Vandenbroucke et al. have reviewed different plasma catalytic processes for TCE abatement [50]. The plasma source that is used in this work is a DC-excited atmospheric pressure glow discharge in a multi-pin-to-plate configuration. This type of plasma source was first proposed by Akishev et al. who used transverse flow stabilization to obtain a uniform glow discharge in a (negative) corona (point-to-plane) electrode geometry [51]. The physics of the corona to-glow transition was studied in detail in previous papers [52,53]. This reactor concept has several desirable features because it can easily be scaled–up, it is cost saving due to the low investment for a DC high voltage source and it allows treating high flow rates at atmospheric pressure and room temperature [54,55]. In this work, the feasibility of combining this multi–pin–to–plate negative DC glow discharge with heterogeneous catalysts for CVOC abatement is investigated in order to enhance the performance of the plasma alone systems. In order to minimize the energy cost of the abatement process, combination of low energy density plasma and moderate catalyst temperature have been examined.

2. Experimental

The experimental set-up (Fig. 1) was described in detail elsewhere [15]. In brief, the plasma source consists of 10 aligned cathode pins (separated by 28 mm) and a single anode plate as counter electrode forming a rectangular duct (40 mm × 9 mm cross section and 400 mm length). The inter-electrode gap in this configuration is 10 mm. A DC power supply (Technix, SR40-R-1200) is used to generate corona/glow discharge at ambient conditions. The discharge voltage and current were varied between 8.0–10.5 kV and 0.04–0.20 mA, respectively.

TCE concentration was controlled by changing feed gas (dry synthetic air–Air Liquide Alphagaz 1) flow rate through a TCE bubbling bottle by using mass flow controllers (MFC). A total air flow rate of 0.5 L/min containing 500 ppm TCE was conveyed in all experiments. A Fourier transform infrared spectrometer (FT-IR) (Bruker, Vertex 70)

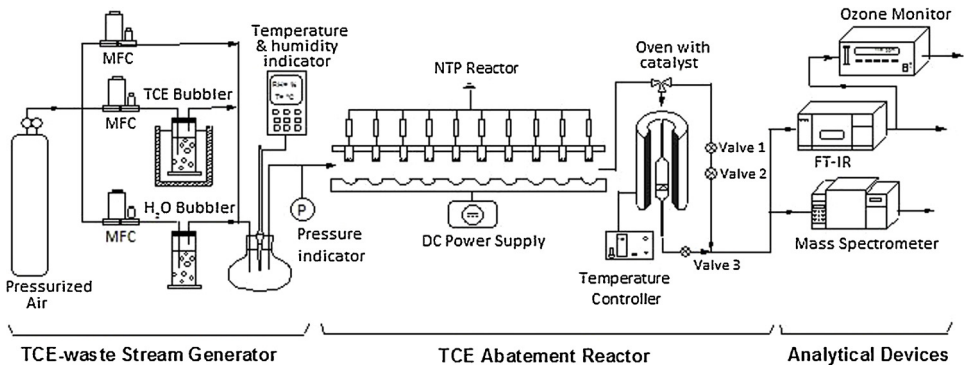

Fig. 1. Schematic diagram of the experimental set-up.

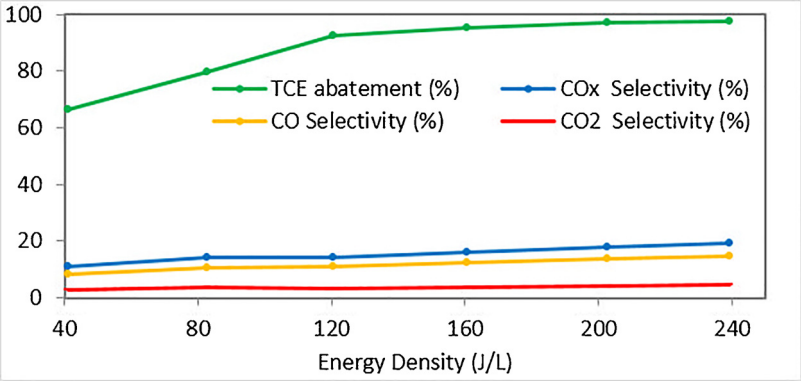

Fig. 2. TCE abatement, CO, CO_2 and CO_x selectivity as a function of the energy density.

and a mass spectrometer (MS) (Hiden, HPR-20 QIC Edwards Vacuum) were used to identify and quantify by-products and TCE abatement. The FTIR spectrometer is equipped with a gas cell of optical length of 20 cm and the resolution of the spectrometer are set at 4 cm^{-1}. The mercury-cadmium-telluride (MCT) detector is used to detect the spectra and it was cooled with liquid nitrogen to ensure operation ability. OPUS (Bruker) software is used to collect and analyze the obtained spectra and these spectra were taken after steady state condition and consisted of 10 averaged measurements. The obtained spectra were measured from 700 to 3045 cm^{-1}.

The quadrupole probe of MS is comprising with a Faraday cup and a secondary electron multiplier (SEM) detector. MASsoft 7 Professional (QGA Professional) software is applied for collecting and displaying data. The qualitative identification of the by-products were achieved using Scan Bargraph mode over the corresponding fragment ions (m/z) with fast response times of less than 150 ms. Depending on the acquisition range (concentration/partial pressure of the trace elements), detectors were chosen to identify the peaks of mass spectra. For instance, in these experiments, Faraday ($1*10^{-5}$ to $1*10^{-8}$ Torr) and SEM ($1*10^{-8}$ to $1*10^{-13}$ Torr) detector identified mass spectra in the range of 0–44 m/z and 45–150 m/z, respectively. Detector voltage of 850 V with electron ionization energy of 70 eV was adopted. An UV ozone detector (Envitec, model 450) was used to monitor the formation of ozone.

Cerium oxide (22,390 Sigma-Aldrich) was calcinated for 4 h at 600 °C under 0.2 L/min flow rate of dry synthetic air. For all tests, 0.5 g of CeO_2 powder mixed with 2.5 g carborundum (SiC-0.105 mm) (EMB 45053-Prolabo) was introduced in a cylindrical Pyrex glass reactor located in a temperature controlled vertical tubular oven. SiC was used to provide uniform flow distribution through the catalyst reactor. The investigated temperature range for catalytic and plasma-catalytic tests was 100–550 °C and 100–300 °C, respectively.

3. Results and discussion

To investigate the performance of the combined plasma–catalytic system, both parts are initially considered separately, i.e. destruction of TCE through the use of NTP and via catalytic oxidation. To evaluate the efficiency of the process the following parameters were estimated:

Discharge power P is the power deposited into the plasma:

$$P = U_{pl} I \tag{1}$$

where U_{pl} is the plasma voltage and I the discharge current.

Energy density (ED) is the energy deposited per unit volume of process gas:

$$ED = \frac{E}{V} = \frac{P}{Q} \tag{2}$$

where E is the energy deposited in the treated volume V and Q is the gas flow rate. The unit of ED is J/L although other units such as kWh/m^3 are also possible.

The TCE abatement is the basic parameter which indicates the relative amount of removed TCE:

$$TCE\ abatement\ (\%) = \frac{[TCE]_{in} - [TCE]_{out}}{[TCE]_{in}} \times 100 \tag{3}$$

where $[TCE]_{in}$ is the initial TCE concentration and $[TCE]_{out}$ the concentration in the effluent. In this work, other terms are also used such as removal efficiency and conversion.

The selectivities of CO, CO_2, CO_x are defined as:

$$S_{CO}(\%) = \frac{[CO]}{2 \times [TCE]_{conv}} \times 100 \tag{4}$$

$$S_{CO_2}(\%) = \frac{[CO_2]}{2 \times [TCE]_{conv}} \times 100 \tag{5}$$

$$S_{CO_x}(\%) = S_{CO} + S_{CO_2} \tag{6}$$

where $[CO]$ and $[CO_2]$ are the concentrations of carbon monoxide and carbon dioxide detected in the effluent gas as a result of TCE oxidation and $[TCE]_{conv}$ is the concentration of TCE converted by the plasma.

The yields of CO and CO_2 and CO_x are defined as follows:

$$Y_{CO}(\%) = \frac{[CO]}{2 \times [TCE]_{in}} \times 100 \tag{7}$$

$$Y_{CO_2}(\%) = \frac{[CO_2]}{2 \times [TCE]_{in}} \times 100 \tag{8}$$

$$Y_{CO_x}(\%) = Y_{CO} + Y_{CO_2} \tag{9}$$

3.1. TCE abatement with NTP alone

Fig. 2 shows the TCE abatement and CO, CO_2 and CO_x selectivity as a function of the energy density for the plasma alone case. Since the discharge is only operated in the corona or glow regime, as expected, with increasing energy density the abatement of TCE increases. At higher energy density, more energetic electrons are produced which trigger the formation of radicals capable of decomposing TCE. For an energy density of 240 J/L the abatement and CO_x selectivity reach a maximum at 97.7% and 19.1%, respectively. This low selectivity is related to the formation of unwanted and toxic by-products such as phosgene (PG) and DCAC [27].

It is important to get insight on the underlying mechanisms and reactions of the removal process, which can yield measures to improve the removal efficiency and CO_x selectivity. The destruction of TCE with NTP takes place through many possible pathways [56]. Electron attachment of TCE, leading to the formation of C_2HCl_2 and a chlorine anion is one of the possible pathways for TCE decomposition. The contribution of the electron attachment of TCE depends on the electron density, number density as well as reaction rate coefficient in the

plasma discharge. However, the electron density of the corona discharge used for this application ($\approx 10^5$-10^6 cm^{-3}) [[56]] is quite low compared with other NTP processes such as dielectric barrier discharges (higher electron density). Additionally, based on the low magnitude of the reaction rate coefficient (1.5×10^{-13} cm^3 $molecule^{-1}$ s^{-1}) found by Vandenbroucke et al. [56], the contribution of this dissociative electron attachment reaction should be limited. Furthermore, according to Magureanu et al. [57] and Urashima et al. [58], the dissociative electron attachment will give a noticeable contribution to the destruction of TCE at rather high concentrations of TCE about 1000 ppm and higher. They suggest that at smaller concentration, TCE oxidation takes place directly by radicals or via oxidation of negative ions. In a study performed by Penetrante et al. [59] shows that for small initial concentrations of TCE in dry air, electrons will mainly attach to oxygen which is believed to be the primary initiation step. Metastable nitrogen molecules are also considered as dominant dissociation species occurring in a NTP destruction process of VOC polluted air streams [60,61]. However, no reaction rate coefficients for TCE with metastable nitrogen have been found in literature.

Although different opinions exist among researchers about the primary initial steps for TCE decomposition (electron impact dissociative attachment/ reactions with radicals/oxidation of negative ions) [57–59,62–64], it is however generally accepted that the chlorine radical chain reaction is the main decomposition mechanism of TCE [59,61,63,65]. In this case, i.e. at the concentration of TCE lower than 1000 ppm, the most probable channels of the TCE destruction are connected with O and OH (specially in humid air) radicals. The reaction of TCE with electrons and (or) O, OH and N_2^* radicals initiates a detachment of Cl^* radicals. In its turn, these radicals destroy the TCE molecules on double C=C bond, giving the appearance of new Cl^* radicals, etc., resulting in the start of a chlorine radical chain reaction [63]. Cl^* addition is faster and occurs more easily than with other radicals owing to the presence of C=C π bond in TCE, [63]. According to Vandenbroucke et al., the ClO^* radical is also an important intermediate which oxidizes TCE [66].

Table 1 shows the by-products of NTP treatment detected with FT-IR and MS. DCAC, PG, CO and CO_2 were observed with both techniques. The decomposition of TCE with NTP led to the formation of PG, DCAC and TCAD as incomplete oxidation products. These results are in agreement with Vandenbroucke et al. [27]. According to Kirkpatrick et al. [67], TCE oxidation with NTP produces a significant amount of DCAC by the following reaction:

$$C_2HCl_3 + ClO^* \rightarrow CHCl_2COCl + Cl^* \quad (10)$$

3.2. TCE abatement with the CeO_2 alone

CeO_2 is a multifunctional rare earth oxide, which possesses excellent physical and chemical properties and has been widely used in several advanced applications such as heterogeneous catalysis [68,69], electrochemistry [70], photochemistry [71] and material science [72]. CeO_2 has been chosen as catalyst due to its unique properties such as a higher oxygen storage/transport capacity [73]. Additionally, the ability to easily shift between reduced and oxidized states (i.e. Ce^{3+}–Ce^{4+}), which results in an increase in oxygen vacancies, leads to an increased catalytic activity [74][21, 22].

Table 1
Detected by-products with NTP.

By-product	Structure	FT-IR	MS	Unwanted
Dichloroacetylchloride(DCAC)	$CHCl_2COCl$	√	√	√
Trichloroacetaldehyde (TCAD)	CCl_3COH	√	√	√
Phosgene (PG)	$COCl_2$	√	√	√√
Hydrogen chloride	HCl	√		
Chlorine	Cl_2		√	
Carbon monoxide	CO	√	√	√
Carbon dioxide	CO_2	√	√	
Ozone	O_3	√		√

Fig. 3 shows the TCE abatement, CO, CO_2 and CO_x selectivity as a function of the temperature of CeO_2. The catalyst activity was evaluated for the temperature range of 100–550 °C. Fig. 3 clearly shows that CeO_2 is not active below 300 °C. Above this temperature, the abatement slightly increases until 450 °C whereafter it sharply increases with increasing temperature. The maximum obtained value of TCE abatement is 90% at 550 °C. CO_x selectivity reaches a plateau (87%) at 450 °C and remains more or less constant with further increase of the temperature. These results prove that high temperature is essential to achieve both high TCE abatement and selectivity.

It is noteworthy to state that the main products found in the catalytic destruction of TCE over CeO_2 are CO_2, CO, H_2O, $COCl_2$ and HCl recorded by both FT-IR and MS and Cl_2 recorded by MS only. In general, it is commonly accepted that the catalytic oxidation process of VOCs over metal oxide catalysts occurs according to the Mars Van Krevelen mechanism where both gas phase oxygen and latice oxygen participate. Dai et al. proposed possible reaction paths of TCE degradation over CeO_2 catalyst [75,76]. Briefly, the formation of intermediate species C_2HCl resulted from the C−Cl bond cleavage during TCE adsorbtion on CeO_2 active sites. This reactive intermediate can be easily further dissociated by CeO_2 and can be totally oxidized by adsorption of oxygen species (O^-), to form final reaction products such as CO_2 and H_2O.

3.3. TCE abatement with post plasma catalytic system

In order to reduce the energy cost of the process, low energy density plasma is used in combination with moderate catalyst temperature. Therefore, the discharge is operated at 40 and 80 J/L and the process was examined for catalyst temperatures between 100–300 °C.

Fig. 4 shows the TCE abatement, CO, CO_2 and CO_x selectivity as a function of catalyst temperature for a fixed energy density of 80 J/L. The abatement increased with around 10% with plasma catalysis (90%) at 100 °C catalyst temperature compared to NTP alone (79.6%). The abatement of TCE in the catalyst alone system operating at the same temperature was negligible. This means that the combination of NTP with CeO_2 induces a synergetic effect on TCE abatement. In order to quantify the observed synergy, a synergy factor f for TCE abatement is used as proposed by Vandenbroucke et al. [15] and defined as follows:

$$f_{TCE} = \frac{(TCE\ abatement)_{plasma-catalysis}}{(TCE\ abatement)_{plasma} + (TCE\ abatement)_{catalyst}} \quad (11)$$

If this value of f_{TCE} exceeds 1, one can conclude that TCE abatement for plasma catalysis is higher than the sum of its individual values for the plasma and catalyst alone which shows a synergetic effect. Table 2 shows that the synergy factor for TCE abatement ranges from 1.15 to 1.04.

Although at low catalyst temperature plasma catalysis improves TCE abatement, at higher temperatures, the abatement however slightly decreases (5%). Hence, the effect of the catalyst temperature on the synergy factor f_{TCE} is much smaller (Table 2). The small decrease of the synergy factor with increasing temperature can possibly be explained by deactivation of the catalyst due to irreversible adsorption of chlorinated by-products on the catalyst surface. It should be noted that the PPC experiment was continuously carried out by increasing the catalyst temperature in steps of 50 °C from 100 °C to 300 °C. Hence, during the experiment at 300 °C it is plausible that a part of the active sites were poisoned by TCE degradation products, already formed during previous experiments, thereby inhibiting the decomposition of TCE. The study of catalyst stability in PPC configuration is necessary to establish the evolution of such a catalyst which is investigated and will

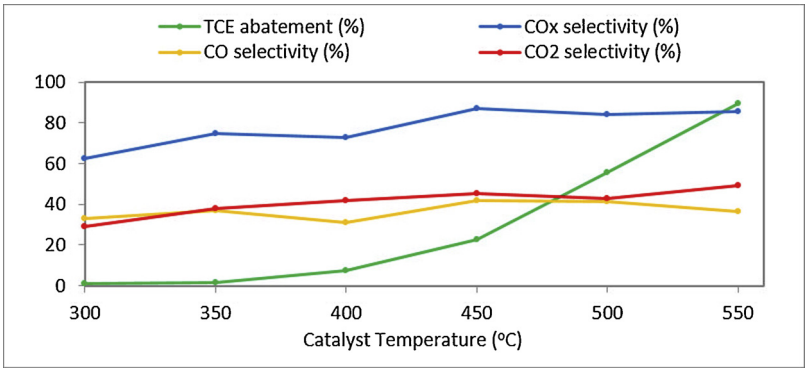

Fig. 3. TCE abatement, CO, CO_2 and CO_x selectivity as a function of the catalyst temperature.

be described in section 3.5.

The PPC system also remarkably enhanced the CO_x selectivity/yield (≈ 90/75%) compared to the plasma alone system (14/9.2%), as shown in Fig. 4. It is noticeable that as the catalyst temperature increases only the CO_x selectivity improves while TCE abatement remains more or less constant. This can be ascribed to the efficient oxidation of oxygenated by-products (DCAC, PG) instead of TCE molecules in the subsequent catalytic reactor because DCAC is more easily destroyed due to its weak bonding energy (3–4 eV) compared to the double bonding energy of TCE (9.45 eV) [61,77–79]. This statement is in agreement with a previous study by Vandenbroucke et al. on plasma catalytic removal of TCE over a MnO_2 catalyst downstream [15]. It was reported that the oxygenated intermediates (DCAC, PG) produced by partial oxidation of TCE in plasma are more reactive than TCE, reach the catalyst surface with a degree of excitation and are more easily decomposed resulting in an improved catalytic performance. This suggests that the polychlorinated intermediates produced by plasma were more susceptible to catalytic oxidation than TCE. Furthermore, a clear synergy was observed for the CO and CO_2 yields (Table 2) which indicates that the plasma catalytic system greatly enhances the selectivity of the process towards total oxidation compared to plasma alone case. The synergy factor f for CO and CO_2 yields are calculated as followed:

$$f_{CO} = \frac{(Y_{CO})_{plasma-catalysis}}{(Y_{CO})_{plasma} + (Y_{CO})_{catalyst}} \quad (12)$$

$$f_{CO_2} = \frac{(Y_{CO_2})_{plasma-catalysis}}{(Y_{CO_2})_{plasma} + (Y_{CO_2})_{catalyst}} \quad (13)$$

The synergy factor for CO and CO_2 yields ranges from 1.64 to 7.11 and 1.52 to 18.05, respectively. The increased CO_x selectivity in the PPC system can be explained by the activated oxidation reactions on the catalyst surface. It is found that p-type oxide semiconductors can effectively decompose ozone which enables the supply of active oxygen species that assist the destruction of the remaining VOC and

Table 2
Synergy factors for plasma catalytic TCE abatement.

Temp (°C)	f_{TCE}		f_{CO}		f_{CO_2}	
	40 J/L	80 J/L	40 J/L	80 J/L	40 J/L	80 J/L
100	1.15	1.11	1.82	1.64	1.57	1.52
150	1.16	1.14	2.84	2.44	7.23	5.85
200	1.12	1.11	3.41	3.01	7.14	7.80
250	1.04	1.09	5.90	4.45	17.65	10.98
300	1.04	1.07	7.11	5.78	18.05	13.14

polychlorinated by-products exiting the plasma reactor [47,80]. Ozone can be cleaved at the catalyst surface, leading to the formation of active oxygen species via [81]:

$$O_3 + * \rightarrow O_2 + O^* \quad (14)$$

$$O_3 + O^* \rightarrow O_2 + O_2^* \quad (15)$$

where * is an active site and O* is the active oxygen specie on the catalyst surface. The active oxygen species may react with remaining VOC or chlorinated by-products adsorbed on the catalyst surface towards total oxidation products (CO_x, H_2O) through Langmuir-Hinshelwood (L-H) mechanism [21], as follows:

$$O^* + VOC_{ads} \rightarrow CO_x + H_2O + * \quad (16)$$

Fig. 5 shows the ozone concentration in the outlet gas of the plasma alone and the PPC system. The use of a catalyst (at 100 °C) downstream of the plasma (operated at 80 J/L) resulted in a decrease of the ozone outlet concentration from 138 to 41 ppm, compared to the plasma alone system. The experiments at an energy density of 80 J/L resulted in a higher ozone production than the 40 J/L case due to the presence of more electrons in the plasma when operating at a higher energy density. An increase of the catalyst temperature further decreased the ozone concentration. Wu et al. reported the ozone decomposition

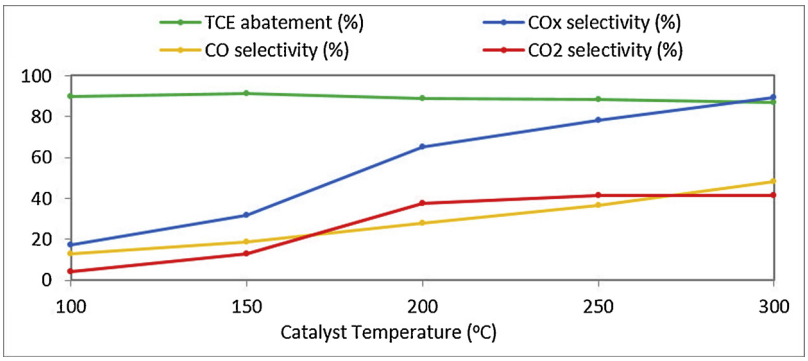

Fig. 4. TCE abatement, CO, CO_2 and CO_x selectivity as a function of the catalyst temperature for energy density 80 J/L.

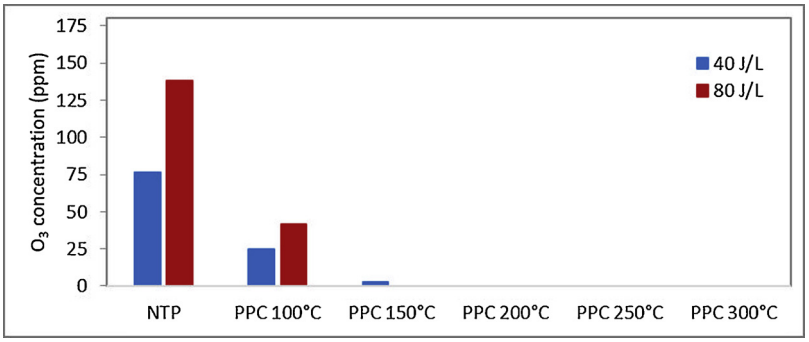

Fig. 5. Ozone outlet concentration of the plasma treated TCE gas in a plasma alone and plasma catalytic (CeO_2) systems for different temperatures.

ability of a CeO_2 catalyst (40 °C) in PPC process [47]. Naydenov et al. have also suggested the production of atomic oxygen species by ozone decomposition on the oxide surface of CeO_2 (10–70 °C) [82]. From these results it can be suggested that ozone dissociates on the catalyst surface to form gas phase molecular oxygen and peroxide groups which enhance the complete oxidation of TCE [15].

However, the decrease in outlet ozone concentration with increasing catalyst/oven temperature could also be attributed to the thermal dissociation of ozone. Therefore, to elucidate the latter assumption, PPC experiments without CeO_2 catalyst (empty glass reactor and with SiC only) have been performed over the temperature range from 100 °C to 300 °C. These results were compared with the CeO_2 and SiC mixture which is the actual experimental condition. The outlet ozone concentration was more or less similar in each PPC experiment especially above 100 °C (Fig. 6) indicating that ozone could be consumed in the oxidation reaction or dissociated by high temperature. Additionally, an increased TCE abatement ranging from 7 to 10% was observed (not shown) in these PPC processes compared to the NTP alone case. It is known that dissociation of ozone into molecular oxygen and atomic oxygen occurs at 100 °C [83]. These molecular/atomic oxygens may react with unreacted TCE, hence promoting higher TCE removal efficiency in each PPC experiment. Nonetheless, the CO_x selectivity is only much higher in the presence of CeO_2 compared to others situations (Fig. 7) showing the importance of the reactive surface. Indeed the VOC removal by plasma catalysis is not only governed by gas phase reactions but also by surface reactions on the catalyst [11]. Teramoto et al. also reported another possible mechanism in which gas phase ozone directly reacts with adsorbed VOCs or chlorinated by-products through an Eley-Rideal (E–R) mechanism [84], as follows:

$$O_3 + VOC_{ads} \rightarrow CO_x + H_2\,O + * \quad (17)$$

However, this phenomenon is only valid if the catalyst acts below 100 °C temperature since O_3 can be decomposed at higher temperatures before interacting with the adsorbed VOCs. Hence, this mechanism can be ruled out in our experimental condition.

It is expected that the increase of the catalyst reactor temperature may increase the thermal decomposition of ozone in the vicinity of the catalyst leading to a decrease in the disposal of O_3 which will be catalytically decomposed on the catalyst. However, at the same time, reactions at the catalyst surface, such as decomposition of ozone and interactions between reactive adsorbed oxygen atoms and TCE and related gaseous polychlorinated by-products, are also accelerated. Higher catalyst temperature promotes the catalyst activity such as high oxygen storage capacity due to its high bulk oxygen mobility and oxygen vacancies. The oxygen storage capacity can be determined by the redox couple of Ce^{4+}/Ce^{3+} [85]. Ceria itself has a certain amount of surface active oxygen species which may contribute to surface

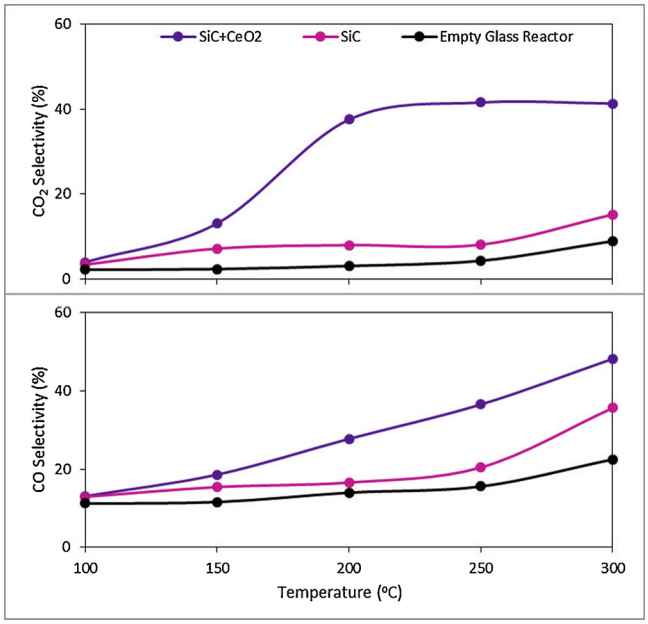

Fig. 7. CO and CO_2 selectivity for the PPC experiment with/without CeO_2 catalyst as a function of operating temperature. ED = 80 J/L.

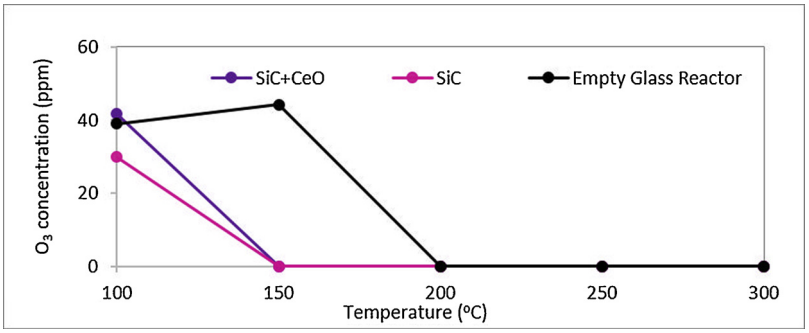

Fig. 6. Ozone outlet concentration for the PPC experiment with/without CeO_2 catalyst as a function of operating temperature. ED = 80 J/L.

reactions. Moreover, CeO_2 can also act as local source/sink of oxygen species which favors the generation of surface adsorbed oxygen species enabling the deep oxidation of the target pollutant/by-products. The increased value of CO and CO_2 selectivity clearly suggests the surface reaction of the plasma processed gaseous polychlorinated by-products as well as the remaining TCE with the active oxygen species on CeO_2 catalyst surface. As previously stated, according to Dai et al., adsorbed oxygen species play a key role for TCE decomposition on CeO_2 catalyst [76]. Therefore, one may conclude that adsorbed VOCs (TCE and by-products) may react with adjacent reactive oxygen species (active O species by O_3 decomposition/lattice O) through L-H mechanism where the resulting oxygen vacancies on the catalyst surface can be replenished by gas phase atomic O formed by thermal dissociation of O_3. The increase of CO_x selectivity with an elevated temperature clearly shows the acceleration of the catalytic activity of CeO_2 with increasing temperature.

3.4. By-product distribution of TCE decomposition

As previously discussed, the use of NTP in combination with a catalyst clearly enhances the CO_x selectivity which reduces the formation of chlorinated by-products. Therefore, it is interesting to identify the chlorinated by-products and to investigate if new products are formed in the PPC system.

Fig. 8 shows the FT-IR analysis of both inlet and outlet streams when plasma is operated at 80 J/L with or without CeO_2 catalyst maintained at 300 °C. The by-products formed by NTP treatment which have already been mentioned in Table1 are identified by carefully comparing these spectra with NIST IR spectra standard reference database. The TCE abatement is calculated by taking the ratio of the integrated surface area of the inlet and outlet band of TCE at 945 cm^{-1} which is not interfered by other by-products IR bands. From Fig. 8 it is clearly evident that plasma catalysis suppresses the unwanted by-products (DCAC, PG and O_3) formed in NTP treatment. Furthermore, two new IR bands appear at 794 and 773 cm^{-1} in minor extent which have been previously ascribed to CCl_4 and $CHCl_3$, respectively [16]. These new C1 chlorinated products may be produced from the reaction of adsorbed chlorinated species with $CHCl_2$ and CCl_3 radicals resulting from the catalytic cleavage of the TCAD and DCAC molecules. As for the formation of NO_2, it was neither detected by the NTP nor by PPC process unlike the work of Nguyen Dinh et al. [17].

The enhanced oxidation in PPC system with increasing catalyst temperature resulted in an increased formation of CO_x and HCl and a decreased formation of DCAC, as shown in Fig. 9 (c) and (d). The increased formation of HCl, compared to the plasma alone system can be explained by the production of oxygen radicals on the catalyst surface, enhancing the rate of the following oxidation reaction:

$$C_2HCl_3 + 4\ O \rightarrow\ 2CO_2 + HCl + Cl_2 \quad (18)$$

The increased phosgene production at a higher catalyst temperature as shown in Fig. 9 (a) is remarkable. A possible explanation is the increased formation of ClO radicals with the catalyst temperature which further reacts with TCE towards phosgene via:

$$Cl_2 + O \rightarrow Cl + ClO \quad (19)$$

$$C_2HCl_3 + ClO \rightarrow COCl_2 + CHCl_2 \quad (20)$$

However, above 200 °C the formation of PG was completely suppressed.

In addition to FT-IR, mass spectra of the inlet and outlet gas streams are also recorded in order to identify additional by-products which have also been mentioned in Table 1. It is important to analyze MS results since the presence of some products cannot be identified with only FT-IR due to the interference of other by-products bands. Additionally, diatomic molecules such as Cl_2 and IR-transparent cannot be identified with FT-IR. Fig. 10 exhibits the mass spectra of inlet and outlet gas streams when plasma is operated at 80 J/L with or without CeO_2 catalyst, where the temperature of the catalyst was maintained at 300 °C. All the peaks in these spectra are identified by comparison to the NIST mass spectral library. The typical characteristic TCE fragment ions, C_2HCl^+ (*m/z*: 60, 62), $C_2HCl_2^+$ (*m/z*: 95, 97, 99) and $C_2HCl_3^+$ (*m/z*: 130, 132, 134, 136), are detected in the inlet TCE gas stream (Fig. 10-a). Fig. 10-b represents the mass spectrum of the outlet gas stream, treated at an energy density of 80 J/L. The detailed mass spectra analysis is described in a previous study [27]. A brief description is however given here. The figure shows a decrease in the abundance of the TCE fragment ions suggesting partial TCE decomposition. Simultaneously some additional peaks were also detected which confirms the formation of polychlorinated by-products due to incomplete oxidation of TCE in the plasma reactor. For instance, the characteristic fragment ions of *m/z* 83, 85 ($CHCl_2^+$), *m/z* 63, 65 ($CClO^+$), *m/z* 48, 50 ($CHCl^+$) can be ascribed to DCAC. The characteristic fragment ions of *m/z* 146, 148 ($C_2HCl_3O^+$), *m/z* 117, 119 ($CCl3^+$), *m/z* 111, 113 ($C_2HCl_2O^+$) can be ascribed to TCAD but also to DCAC. The characteristic fragment ions

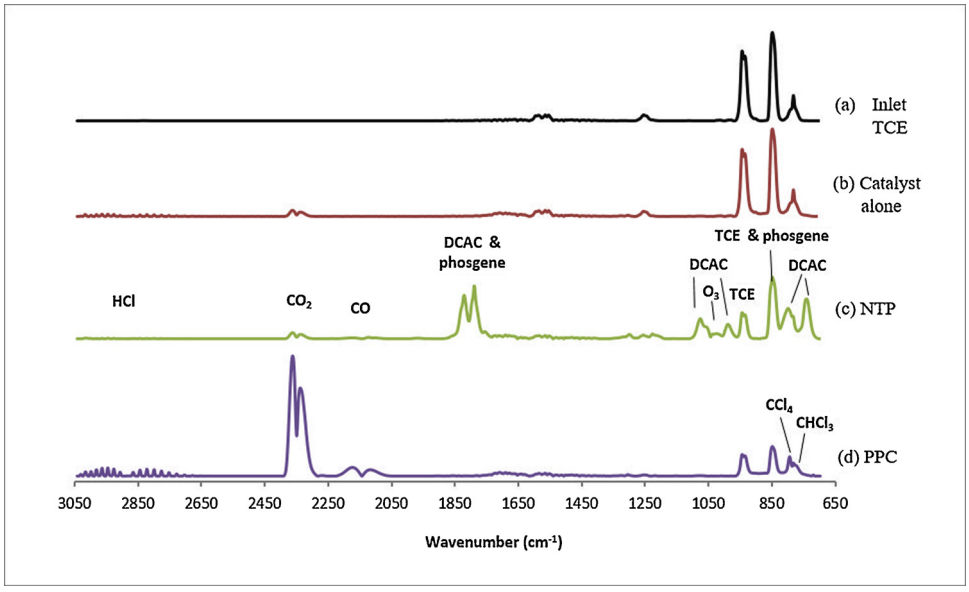

Fig. 8. FT-IR spectra of (a) inlet TCE, (b) Catalyst alone (300 °C), (c) NTP (80 J/L) and (d) PPC (80 J/L- 300 °C).

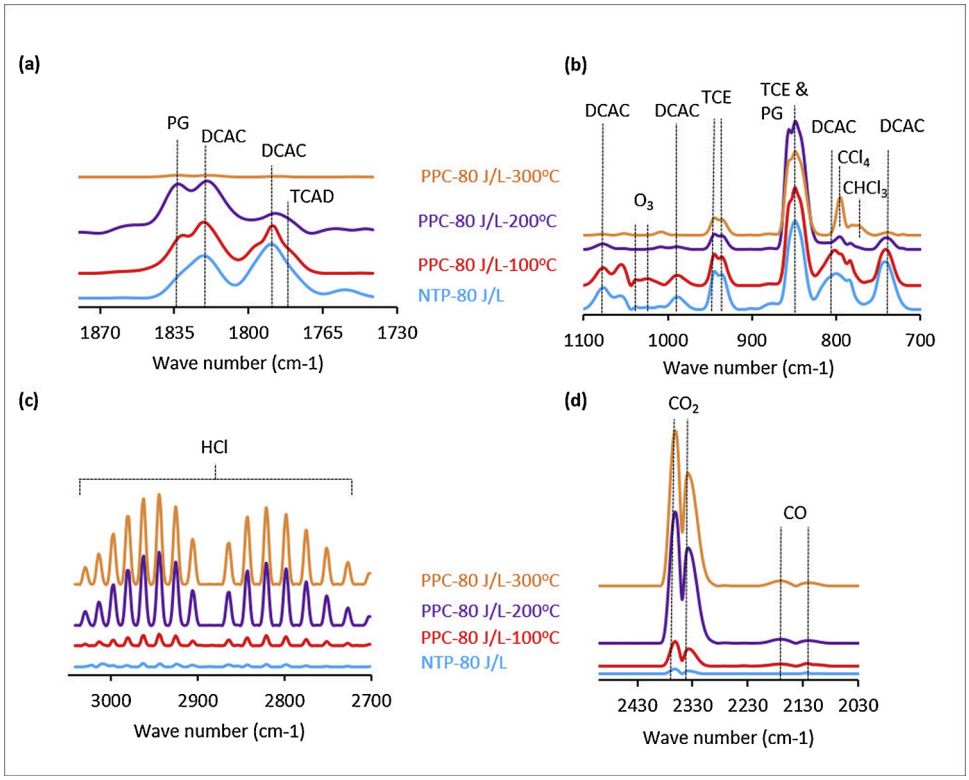

Fig. 9. FT-IR spectra of the gaseous phase at the exit of the catalytic reactor at different temperature between (a) 700–1100, (b) 1730–1880, (c) 2010–2430 and (d) 2700–3000 cm^{-1}.

of *m/z* 82, 84 (CCl_2^+) can be ascribed to TCAD only. However, the lower intensity indicates low content of TCAD formation. Phosgene is also detected by the characteristic fragment ions at 63 and 65 *m/z* ($CO^{35}Cl^+$ and $CO^{37}Cl^+$) present in the mass spectrum of the outlet gas. The mass spectrum of the outlet gas revealed the formation of Cl_2 by the peaks at *m/z* 70 ($^{35}Cl^{35}Cl^+$), 72 ($^{35}Cl^{37}Cl^+$) and 74 ($^{37}Cl^{37}Cl^+$). The formation of HCl and CO_2 are established by the peaks in mass spectrum at *m/z* of 36 ($H^{35}Cl^+$) and 44 (CO_2^+) which is not shown here. Fig. 10-c shows the mass spectra in case of plasma catalysis operated at 80 J/L and 300 °C. The suppression of all detected chlorinated by-products except Cl_2 molecules is clearly evident by the decrease in the abundance of corresponding fragment ions in this figure. Nonetheless, trace amounts of $CHCl_3$ and CCl_4 have been confirmed by the characteristic fragment ions of *m/z* 83, 85 ($CHCl_2^+$) and 117, 119 (CCl_3^+), respectively.

3.5. Stability of the catalyst

Next to activity and selectivity, stability is also an important feature of the catalyst, especially for practical applications. In this regard, a

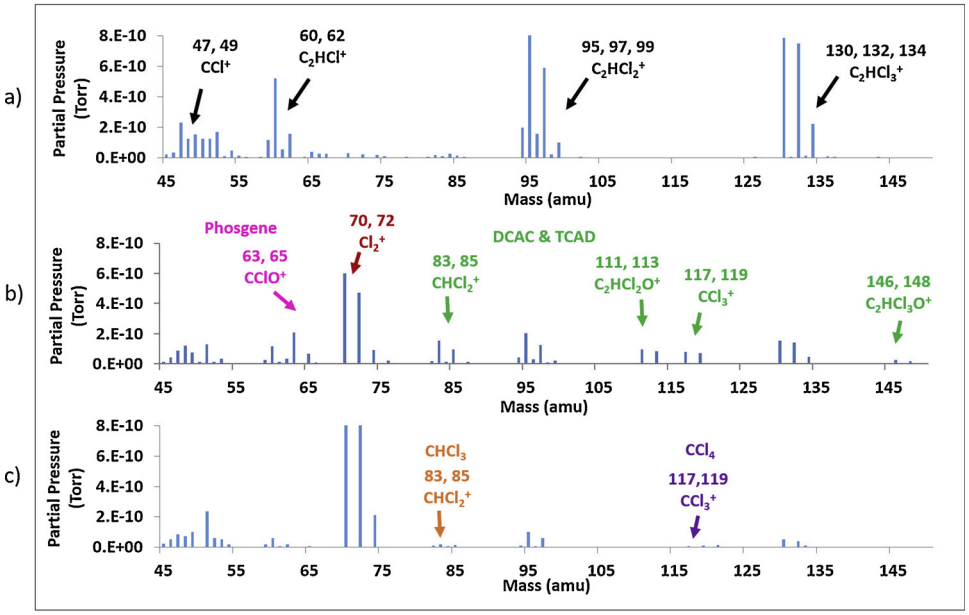

Fig. 10. Mass spectra of a) TCE inlet, b) plasma alone (80 J/L) and c) plasma catalysis (80 J/L-300 °C).

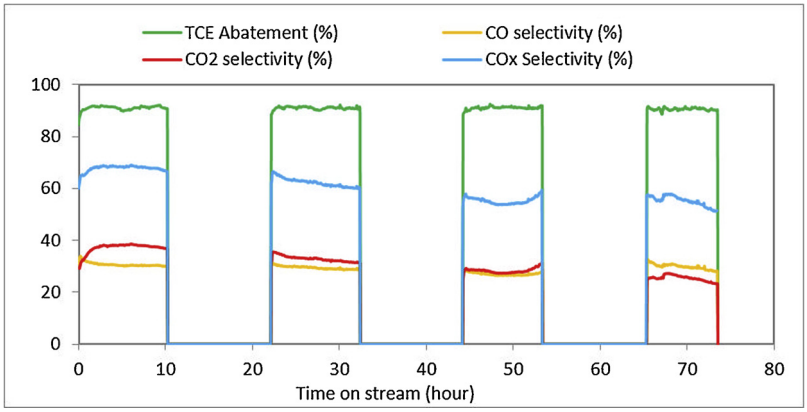

Fig. 11. Stability test of catalyst.

stability test of the plasma catalytic process has been performed at low energy density (80 J/L) and moderate catalyst temperature (200 °C).

The experiment was carried out over 4 days with a daily startup–-shutdown. During the 4 days run, TCE waste gas stream (C_{TCE} = 500 ppm, Q = 0.5 L/min) was treated with plasma catalysis each day for about 10 h (total time on stream was around 40 h). During the shutdown period (at night), plasma was turned off and a 0.2 L/min air flow rate was passed through the catalytic bed. Fig. 11 displays the TCE abatement, CO, CO_2 and CO_x selectivities obtained with the stability test of plasma catalysis. Both plasma and catalyst are found to be stable over the tested time on stream. The experiment demonstrated that plasma catalysis maintained the same initial activity over 40 h in terms of TCE abatement (90%). However, CO_x selectivity decreased around 13% during the reaction period. This could be attributed to the deactivation of the catalyst surface either by chlorination or by blocking of active sites [75,76].

Notably, roughly a similar amount of TCE abatement was observed in each PPC test regardless the type of material introduced downstream (discussed in Section 3.3) and a high CO_x selectivity was observed only in the presence of the catalyst (Fig. 7). Moreover, with time on stream TCE abatement is not altered but the CO_x selectivities decrease. This may suggest that with the assistance of NTP, CeO_2 (at lower catalyst temperature) may be enough activated to only selectively react with hazardous polychlorinated by-products (which need less energy to oxidise than TCE) to form the desired product (CO_2).

4. Conclusions

The abatement of TCE from dry air was investigated by a combined use of a multi-pin-to-plate negative DC corona/glow discharge with a CeO_2 catalyst downstream.

NTP enables catalyst activation at lower temperature. The ozone degradation capacity combined with high oxygen storage capacity of the CeO_2 catalyst may contribute to the generation of active oxygen species and the enhancement of oxygen mobility enabling the deep oxidation of the unreacted TCE and the polychlorinated by-products exiting from NTP leading to an improved TCE abatement and CO_x selectivities. It was found that the polychlorinated intermediates produced by plasma were more susceptible to catalytic oxidation than TCE.

By examining the effect of catalyst temperature, it was observed that low energy density plasma in combination with moderate catalyst temperature successfully abated dilute TCE in air streams. Hence, this plasma catalysis route shows great potential as air pollution control technology for low concentrated VOC air streams at a lower energy cost.

Furthermore, a long term test to evaluate the stability of CeO_2 catalyst has also been successfully performed.

Acknowledgements

The research has been partially supported by an Interreg V France-Wallonie-Vlaanderen project entitled “DepollutAir” and a PICS (Preparation of catalysts and catalytic depollution assisted by plasma) from CNRS is acknowledged for financial support. M. Mora, C. Jimenez-Sanchidrián and F.J. Romero-Salguero acknowledges funding from Junta de Andalucia (P10-FQM-6181), Ministry of Science and Innovation (MAT 2013-44463-R) and Fondos Feder.

References

[1] P. Vineis, F. Forastiere, G. Hoek, M. Lipsett, Outdoor air pollution and lung cancer: recent epidemiologic evidence, Int. J. Cancer 111 (2004) 647–652.
[2] T. Yamamoto, K. Ramaanathan, P.A. Lawless, D.S. Ensor, J.R. Newsome, N. Plaks, R. G.H, Control of volatile organic compounds by an AC energized ferroelectric pellet reactor and a pulsed corona reactor, IEEE Trans. Ind. Appl. 28 (1992) 528–534.
[3] C.M. Nunez, G.H. Ramsey, W.H. Ponder, J.H. Abbott, L.E. Hamel, P.H. Kariher, Corona destruction: an innovative control technology for VOCs and air toxics, Air Waste 43 (1993) 242–247.
[4] A. Ogata, N. Shintani, K. Mizuno, S. Kushiyama, T. Yamamoto, Decomposition of benzene using a nonthermal plasma reactor packed with ferroelectric pellets, IEEE Trans. Ind. Appl. 35 (1999) 753–759.
[5] J.S. Chang, Next generation integrated electrostatic gas cleaning systems, J. Electrostat. 57 (2003) 273–291.
[6] Y. Dan, D.S. Gao, G. Yu, X.L. Shen, F. Gu, Investigation of the treatment of particulate matter from gasoline engine exhaust using non-thermal plasma, J. Hazard. Mater. 127 (2005) 149–155.
[7] M. Laroussi, Low temperature plasma-based sterilization: overview and state-of-the-art, Plasma Process. Polym. 2 (2005) 391–400.
[8] J. Van Durme, J. Dewulf, C. Leys, H. Van Langenhove, Combining non-thermal plasma with heterogeneous catalysis in waste gas treatment: a review, Appl. Catal. B-Environ. 78 (2008) 324–333.
[9] H.L. Chen, H.M. Lee, S.H. Chen, M.B. Chang, S.J. Yu, S.N. Li, Removal of volatile organic compounds by single-stage and two-stage plasma catalysis systems: a review of the performance enhancement mechanisms, current status, and suitable applications, Environ. Sci. Technol. 43 (2009) 2216–2227.
[10] A.M. Vandenbroucke, R. Morent, N. De Geyter, C. Leys, Non-thermal plasmas for non-catalytic and catalytic VOC abatement, J. Hazard. Mater. 195 (2011) 30–54.
[11] S. Sultana, A.M. Vandenbroucke, C. Leys, N. De Geyter, R. Morent, Abatement of VOCs with alternate adsorption and plasma-assisted regeneration: a review, Catalysts 5 (2015) 718–746.
[12] H.H. Kim, A. Ogata, S. Futamura, Effect of different catalysts on the decomposition of VOCS using flow-type plasma-driven catalysis, IEEE Trans. Plasma Sci. 34 (2006) 984–995.
[13] R. Morent, J. Dewulf, N. Steenhaut, C. Leys, H. Van Langenhove, Hybrid plasma-catalyst system for the removal of trichloroethylene in air, J. Adv. Oxid. Technol. 9 (2006) 53–58.
[14] T. Oda, T. Takahashi, S. Kohzuma, Decomposition of dilute trichloroethylene by using nonthermal plasma processing-frequency and catalyst effects, IEEE Trans. Ind. Appl. 37 (2001) 965–970.
[15] A.M. Vandenbroucke, M. Mora, C. Jimenez-Sanchidrian, F.J. Romero-Salguero, N. De Geyter, C. Leys, R. Morent, TCE abatement with a plasma-catalytic combined system using MnO2 as catalyst, Appl. Catal. B-Environ. 156 (2014) 94–100.
[16] M.T. Nguyen Dinh, J.M. Giraudon, J.F. Lamonier, A. Vandenbroucke, N. De Geyter, C. Leys, R. Morent, Plasma-catalysis of low TCE concentration in air using LaMnO3 + delta as catalyst, Appl. Catal. B-Environ. 147 (2014) 904–911.
[17] M.T.N. Dinh, J.M. Giraudon, A.M. Vandenbroucke, R. Morent, N. De Geyter,

J.F. Lamonier, Post plasma-catalysis for total oxidation of trichloroethylene over Ce-Mn based oxides synthesized by a modified "redox-precipitation route", Appl. Catal. B-Environ. 172 (2015) 65–72.
[18] U. Roland, F. Holzer, A. Poppl, F.D. Kopinke, Combination of non-thermal plasma and heterogeneous catalysis for oxidation of volatile organic compounds Part 3. Electron paramagnetic resonance (EPR) studies of plasma-treated porous alumina, Appl. Catal. B-Environ. 58 (2005) 227–234.
[19] C. Subrahmanyam, Catalytic non-thermal plasma reactor for total oxidation of volatile organic compounds, Indian J. Chem. Sec. A-Inorg. Bio-Inorg. Phys. Theor. & Anal. Chem. 48 (2009) 1062–1068.
[20] T. Zhu, J. Li, W.J. Liang, Y.Q. Jin, Synergistic effect of catalyst for oxidation removal of toluene, J. Hazard. Mater. 165 (2009) 1258–1260.
[21] J. Van Durme, J. Dewulf, W. Sysmans, C. Leys, H. Van Langenhove, Efficient toluene abatement in indoor air by a plasma catalytic hybrid system, Appl. Catal. B-Environ. 74 (2007) 161–169.
[22] H.B. Huang, D.Q. Ye, X.J. Guan, The simultaneous catalytic removal of VOCs and O-3 in a post-plasma, Catal. Today 139 (2008) 43–48.
[23] A. Ogata, K. Saito, H.H. Kim, M. Sugasawa, H. Aritani, H. Einaga, Performance of an ozone decomposition catalyst in hybrid plasma reactors for volatile organic compound removal, Plasma Chem. Plasma Process. 30 (2010) 33–42.
[24] J. Van Durme, J. Dewulf, W. Sysmans, C. Leys, H. Van Langenhove, Abatement and degradation pathways of toluene in indoor air by positive corona discharge, Chemosphere 68 (2007) 1821–1829.
[25] M. Magureanu, N.B. Mandache, V.I. Parvulescu, C. Subrahmanyam, A. Renken, L. Kiwi-Minsker, Improved performance of non-thermal plasma reactor during decomposition of trichloroethylene: optimization of the reactor geometry and introduction of catalytic electrode, Appl. Catal. B-Environ. 74 (2007) 270–277.
[26] J.P. Borra, A. Goldman, M. Goldman, D. Boulaud, Electrical discharge regimes and aerosol production in point-to-plane dc high-pressure cold plasmas: aerosol production by electrical discharges, J. Aerosol Sci. 29 (1998) 661–674.
[27] A.M. Vandenbroucke, D. Minh Tuan Nguyen, J.-M. Giraudon, R. Morent, N. De Geyter, J.-F. Lamonier, C. Leys, Qualitative by-product identification of plasma-assisted TCE abatement by mass spectrometry and fourier-transform infrared spectroscopy, Plasma Chem. Plasma Process. 31 (2011) 707–718.
[28] K. Abedi, F. Ghorbani-Shahna, B. Jaleh, A. Bahrami, R. Yarahmadi, Enhanced performance of non-thermal plasma coupled with TiO2/GAC for decomposition of chlorinated organic compounds: influence of a hydrogen-rich substance, J. Environ. Health Sci. Eng. 12 (2014).
[29] A.M. Harling, H.H. Kim, S. Futamura, J.C. Whitehead, Temperature dependence of plasma-catalysis using a nonthermal, atmospheric pressure packed bed; the destruction of benzene and toluene, J. Phys. Chem. C 111 (2007) 5090–5095.
[30] S. Ojala, S. Pitkaaho, T. Laitinen, N.N. Koivikko, R. Brahmi, J. Gaalova, L. Matejova, A. Kucherov, S. Paivarinta, C. Hirschmann, T. Nevanpera, M. Riihimaki, M. Pirila, R.L. Keiski, Catalysis in VOC abatement, Top. Catal. 54 (2011) 1224–1256.
[31] B. Mendyka, A. Musialikpiotrowska, K. Syczewska, Effect of chlorine compounds on the deactivation of platinum catalysts, Catal. Today 11 (1992) 597–610.
[32] S. Imamura, Catalytic decomposition of halogenated organic-compounds and deactivation of the catalysts, Catal. Today 11 (1992) 547–567.
[33] J. Grams, J. Goralski, P. Kwintal, ToF-SIMS studies of the regeneration of Pd/TiO2 catalyst used in hydrodechlorination process, Int. J. Mass Spectrom. 292 (2010) 1–6.
[34] J.J. Spivey, complete catalytic-oxidation of volatile organics, Ind. Eng. Chem. Res. 26 (1987) 2165–2180.
[35] S.K. Agarwal, J.J. Spivey, J.B. Butt, Catalyst deactivation during deep oxidation of CHLOROHYDROCARBONS, Appl.Catal. A-Gen. 82 (1992) 259–275.
[36] R. Rachapudi, P.S. Chintawar, H.L. Greene, Aging and structure activity characteristics of CR-ZSM-5 catalysts during exposure to chlorinated VOCs, J. Catal. 185 (1999) 58–72.
[37] M.C. Alvarez-Galvan, V. O'Shea, J.L.G. Fierro, P.L. Arias, Alumina-supported manganese- and manganese-palladium oxide catalysts for VOCs combustion, Catal. Commun. 4 (2003) 223–228.
[38] E. Diaz, S. Ordonez, A. Vega, J. Coca, Catalytic combustion of hexane over transition metal modified zeolites NaX and CaA, Appl. Catal. B-Environ. 56 (2005) 313–322.
[39] D. Dobber, D. Kiessling, W. Schmitz, G. Wendt, MnOx/ZrO2 catalysts for the total oxidation of methane and chloromethane, Appl. Catal. B-Environ. 52 (2004) 135–143.
[40] P. Zimmer, A. Tschöpe, R. Birringer, Temperature-programmed reaction spectroscopy of ceria- and Cu/ceria-supported oxide catalyst, J. Catal. 205 (2002) 339–345.
[41] B. Skårman, D. Grandjean, R.E. Benfield, A. Hinz, A. Andersson, L. Reine Wallenberg, Carbon monoxide oxidation on nanostructured CuOx/CeO2 composite particles characterized by HREM, XPS, XAS, and high-energy diffraction, J. Catal. 211 (2002) 119–133.
[42] B. de Rivas, R. López-Fonseca, J.R. González-Velasco, J.I. Gutiérrez-Ortiz, On the mechanism of the catalytic destruction of 1,2-dichloroethane over Ce/Zr mixed oxide catalysts, J. Mol. Catal. A Chem. 278 (2007) 181–188.
[43] B. de Rivas, C. Sampedro, R. Lopez-Fonseca, M.A. Gutierrez-Ortiz, J.I. Gutierrez-Ortiz, Low-temperature combustion of chlorinated hydrocarbons over CeO2/H-ZSM5 catalysts, Appl. Catal. A-Gen. 417 (2012) 93–101.
[44] L. Jiang, G. Nie, R. Zhu, J. Wang, J. Chen, Y. Mao, Z. Cheng, W.A. Anderson, Efficient degradation of chlorobenzene in a non-thermal plasma catalytic reactor supported on CeO2/HZSM-5 catalysts, J. Environ. Sci. China (China) 55 (2017) 266–273.
[45] H.-X. Ding, A.-M. Zhu, F.-G. Lu, Y. Xu, J. Zhang, X.-F. Yang, Low-temperature plasma-catalytic oxidation of formaldehyde in atmospheric pressure gas streams, Journal of Phys. D-Appl. Phys. 39 (2006) 3603–3608.
[46] R.Y. Zhu, Y.B. Mao, L.Y. Jiang, J.M. Chen, Performance of chlorobenzene removal in a nonthermal plasma catalysis reactor and evaluation of its byproducts, Chem. Eng. J. 279 (2015) 463–471.
[47] J. Wu, Y. Huang, Q. Xia, Z. Li, Decomposition of toluene in a plasma catalysis system with NiO, MnO2, CeO2, Fe2O3, and CuO catalysts, Plasma Chem. Plasma Process. 33 (2013) 1073–1082.
[48] I. Rusyn, W.A. Chiu, L.H. Lash, H. Kromhout, J. Hansen, K.Z. Guyton, Trichloroethylene: mechanistic, epidemiologic and other supporting evidence of carcinogenic hazard, Pharmacol. Ther. 141 (2014) 55–68.
[49] L.H. Lash, W.A. Chiu, K.Z. Guyton, I. Rusyn, Trichloroethylene biotransformation and its role in mutagenicity, carcinogenicity and target organ toxicity, Mutat. Res. Mutat. Res. 762 (2014) 22–36.
[50] A.M. Vandenbroucke, R. Morent, N. De Geyter, C. Leys, Decomposition of trichloroethylene with plasma-catalysis: a review, J. Adv. Oxid. Technol. 14 (2011) 165–173.
[51] Y.S. Akishev, A.A. Deryugin, I.V. Kochetov, A.P. Napartovich, N.I. Trushkin, DC glow discharge in air flow at atmospheric pressure in connection with waste gases treatment, J. Phys. D-Appl. Phys. 26 (1993) 1630–1637.
[52] Y.S. Akishev, M.E. Grushin, I.V. Kochetov, A.P. Napartovich, M.V. Pan'kin, N.I. Trushkin, Transition of a multipin negative corona in atmospheric air to a glow discharge, Plasma Phys. Rep. 26 (2000) 157–163.
[53] Y. Akishev, O. Goossens, T. Callebaut, C. Leys, A. Napartovich, N. Trushkin, The influence of electrode geometry and gas flow on corona-to-glow and glow-to-spark threshold currents in air, J. Phys. D-Appl. Phys. 34 (2001) 2875–2882.
[54] R. Morent, C. Leys, Ozone generation in air by a DC-excited multi-pin-to-plane plasma source, Ozone-Sci. Eng. 27 (2005) 239–245.
[55] R. Vertriest, R. Morent, J. Dewulf, C. Leys, H. Van Langenhove, Multi-pin-to-plate atmospheric glow discharge for the removal of volatile organic compounds in waste air, Plasma Sources Sci. Technol. 12 (2003) 412–416.
[56] A.M. Vandenbroucke, R. Aerts, W. Van Gaens, N. De Geyter, C. Leys, R. Morent, A. Bogaerts, Modeling and experimental study of trichloroethylene abatement with a negative direct current corona discharge, Plasma Chem. Plasma Process. 35 (2015) 217–230.
[57] M. Magureanu, N.B. Mandache, V.I. Parvulescu, Chlorinated organic compounds decomposition in a dielectric barrier discharge, Plasma Chem. Plasma Process. 27 (2007) 679–690.
[58] K. Urashima, J.S. Chang, Removal of volatile organic compounds from air streams and industrial flue gases by non-thermal plasma technology, IEEE Trans. Dielectr. Electr. Insul. 7 (2000) 602–614.
[59] B.M. Penetrante, M.C. Hsiao, J.N. Bardsley, B.T. Merritt, G.E. Vogtlin, A. Kuthi, C.P. Burkhart, J.R. Bayless, Identification of mechanisms for decomposition of air pollutants by non-thermal plasma processing, Plasma Sources Sci. Technol. 6 (1997) 251–259.
[60] T. Callebaut, I. Kochetov, Y. Akishev, A. Napartovich, C. Leys, Numerical simulation and experimental study of the corona and glow regime of a negative pin-to-plate discharge in flowing ambient air, Plasma Sources Sci. Technol. 13 (2004) 245–250.
[61] S.B. Han, T. Oda, Decomposition mechanism of trichloroethylene based on by-product distribution in the hybrid barrier discharge plasma process, Plasma Sources Sci. Technol. 16 (2007) 413–421.
[62] D. Evans, L.A. Rosocha, G.K. Anderson, J.J. Coogan, M.J. Kushner, Plasma remediation of trichloroethylene in silent discharge plasmas, J. Appl. Phys. 74 (1993) 5378–5386.
[63] S.A. Vitale, K. Hadidi, D.R. Cohn, P. Falkos, The effect of a carbon-carbon double bond on electron beam-generated plasma decomposition of trichloroethylene and 1,1,1-trichloroethane, Plasma Chem. Plasma Process. 17 (1997) 59–78.
[64] T. Yamamoto, S. Futamura, Nonthermal plasma processing for controlling volatile organic compounds, Combust. Sci. Technol. 133 (1998) 117–133.
[65] L. Prager, H. Langguth, S. Rummel, R. Mehnert, Electron-beam degradation of chlorinated hydrocarbons in air, Radiat. Phys. Chem. 46 (1995) 1137–1142.
[66] A.M. Vandenbroucke, R. Aerts, W. Van Gaens, N. De Geyter, C. Leys, R. Morent, A. Bogaerts, Modeling and experimental study of trichloroethylene abatement with a negative direct current corona discharge, Plasma Chem. Plasma Process. (2014).
[67] M.J. Kirkpatrick, W.C. Finney, B.R. Locke, Chlorinated organic compound removal by gas phase pulsed streamer corona electrical discharge with reticulated vitreous carbon electrodes, Plasmas Polym. 8 (2003) 165–177.
[68] D. Delimaris, T. Ioannides, VOC oxidation over MnOx-CeO2 catalysts prepared by a combustion method, Appl. Catal. B-Environ. 84 (2008) 303–312.
[69] X. Tang, J. Chen, X. Huang, Y. Xu, W. Shen, Pt/MnOx-CeO2 catalysts for the complete oxidation of formaldehyde at ambient temperature, Appl. Catal. B-Environ. 81 (2008) 115–121.
[70] C.O. Avellaneda, M.A.C. Berton, L.O.S. Bulhoes, Optical and electrochemical properties of CeO2 thin film prepared by an alkoxide route, Sol. Energy Mater. Sol. Cells 92 (2008) 240–244.
[71] R.X. Li, S. Yabe, M. Yamashita, S. Momose, S. Yoshida, S. Yin, T. Sato, Synthesis and UV-shielding properties of ZnO- and CaO-doped CeO(2) via soft solution chemical process, Solid State Ion. 151 (2002) 235–241.
[72] X.D. Feng, D.C. Sayle, Z.L. Wang, M.S. Paras, B. Santora, A.C. Sutorik, T.X.T. Sayle, Y. Yang, Y. Ding, X.D. Wang, Y.S. Her, Converting ceria polyhedral nanoparticles into single-crystal nanospheres, Science 312 (2006) 1504–1508.
[73] V. Pitchon, F. Garin, O. Maire, Influence of the surrounding atmosphere upon the catalytic performances of three-way catalysts, Appl. Catal. A-Gen. 149 (1997) 245–256.
[74] G. Balducci, M.S. Islam, J. Kaspar, P. Fornasiero, M. Graziani, Bulk reduction and oxygen migration in the ceria-based oxides, Chem. Mater. 12 (2000) 677–681.
[75] Q.G. Dai, X.Y. Wang, G.Z. Lu, Low-temperature catalytic destruction of chlorinated

VOCs over cerium oxide, Catal. Commun. 8 (2007) 1645–1649.
[76] Q.G. Dai, X.Y. Wang, G.Z. Lu, Low-temperature catalytic combustion of trichloroethylene over cerium oxide and catalyst deactivation, Appl. Catal. B-Environ. 81 (2008) 192–202.
[77] S. Futamura, A.H. Zhang, T. Yamamoto, The dependence of nonthermal plasma behavior of VOCs on their chemical structures, J. Electrostat. 42 (1997) 51–62.
[78] T. Oda, K. Yamaji, T. Takahashi, Decomposition of dilute trichloroethylene by nonthermal plasma processing - Gas flow rate, catalyst, and ozone effect, IEEE Trans. Ind. Appl. 40 (2004) 430–436.
[79] T. Yamamoto, VOC decomposition by nonthermal plasma processing - A new approach, J. Electrostat. 42 (1997) 227–238.
[80] B. Dhandapani, S.T. Oyama, Gas phase ozone decomposition catalysts, Appl. Catal. B-Environ. 11 (1997) 129–166.
[81] W. Li, G.V. Gibbs, S.T. Oyama, Mechanism of ozone decomposition on a manganese oxide catalyst. I. In situ Raman spectroscopy and ab initio molecular orbital calculations, J. Am. Chem. Soc. 120 (1998) 9041–9046.
[82] A. Naydenov, R. Stoyanova, D. Mehandjiev, Ozone decomposition and CO oxidation on CeO2, J. Mol. Catal. A-Chem. 98 (1995) 9–14.
[83] https://authors.library.caltech.edu/42670/1/WULpnas27.pdf.
[84] Y. Teramoto, H.-H. Kim, N. Negishi, A. Ogata, The role of ozone in the reaction mechanism of a bare zeolite-plasma hybrid system, Catalysts 5 (2015) 838–850.
[85] X.B. Zhu, X. Gao, R. Qin, Y.X. Zeng, R.Y. Qu, C.H. Zheng, X. Tu, Plasma-catalytic removal of formaldehyde over Cu-Ce catalysts in a dielectric barrier discharge reactor, Appl. Catal. B-Environ. 170 (2015) 293–300.